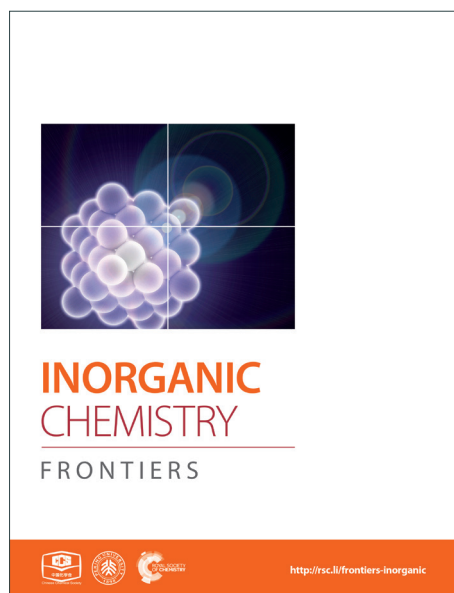
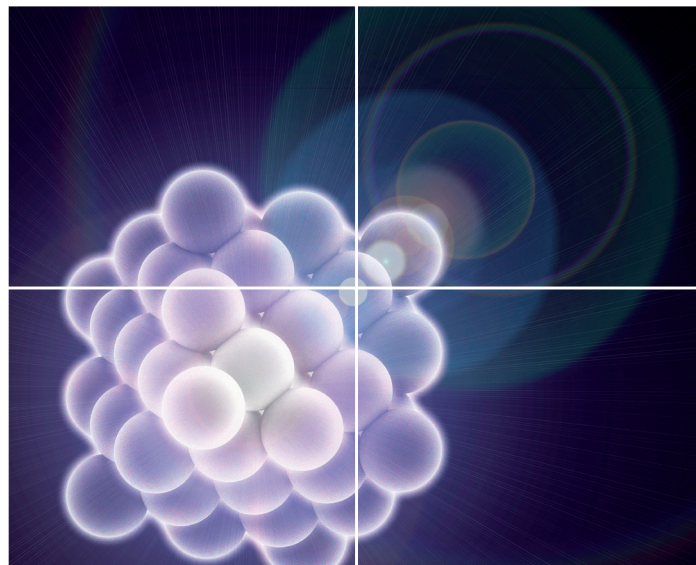


# INORGANIC CHEMISTRY

FRONTIERS

Accepted Manuscript



This is an *Accepted Manuscript*, which has been through the Royal Society of Chemistry peer review process and has been accepted for publication.

*Accepted Manuscripts* are published online shortly after acceptance, before technical editing, formatting and proof reading. Using this free service, authors can make their results available to the community, in citable form, before we publish the edited article. We will replace this *Accepted Manuscript* with the edited and formatted *Advance Article* as soon as it is available.

You can find more information about *Accepted Manuscripts* in the [Information for Authors](#).

Please note that technical editing may introduce minor changes to the text and/or graphics, which may alter content. The journal's standard [Terms & Conditions](#) and the [Ethical guidelines](#) still apply. In no event shall the Royal Society of Chemistry be held responsible for any errors or omissions in this *Accepted Manuscript* or any consequences arising from the use of any information it contains.

Cite this: DOI: 10.1039/c0xx00000x

www.rsc.org/xxxxxx

Review

# Heteroatom-doped carbons: synthesis, chemistry and application in lithium/sulphur battery

Sheng S. Zhang<sup>a\*</sup>

Received (in XXX, XXX) Xth XXXXXXXXXX 20XX, Accepted Xth XXXXXXXXXX 20XX

DOI: 10.1039/b000000x

Doping of heteroatoms into carbon not only changes the electronic distribution but also creates surface functional groups. These changes prove to enhance the chemical adsorption of carbon to sulphur species, and have been intensively investigated to sequester soluble lithium polysulphide in the cathode of lithium/sulphur (Li/S) batteries. The chemical adsorption varies with the type, valence state and content of heteroatoms in a complicated manner. In this review, the syntheses of heteroatom-doped carbons as well as their applications and mechanism in the Li/S batteries are highlighted and discussed with focus on oxygen, sulphur, nitrogen and their mixtures.

## 1. Introduction

The development of lithium/sulphur (Li/S) batteries faces grand challenges in relation to the dissolution of lithium polysulphide (PS,  $\text{Li}_2\text{S}_n$  with  $n>2$ ) in organic electrolytes. By its nature, PS dissolution is intrinsically unavoidable and essential for the effective utilization and fast reaction kinetics of insulating sulphur species.<sup>1</sup> The PS dissolution has been identified to be the source for a number of known problems, including low energy efficiency, fast self-discharge, severe Li corrosion, and poor safety of Li/S batteries. Aiming to solve these problems, researchers have focused on two directions of (1) trapping the soluble PS from diffusing out of the cathode and (2) protecting the Li anode from reacting with the dissolved PS.<sup>2,3</sup> In efforts to trap the soluble PS within the cathode, a number of strategies have been attempted and investigated, including sulphur-carbon (S-C) composites, metal oxides and conducting polymers for advanced materials; dual-layer structured cathode (or called PS-absorbing interlayer) and PS diffusion blocking layer for improved cell configurations.<sup>4-8</sup> Among these strategies, the S-C composites have been most intensively studied due to the wide variation and low cost of commercial and synthetic carbons. The trapping of PS by the S-C composites is typically a combined effect of physical absorption (PAB) and chemical adsorption (CAD). The PAB traps PS through weak Van der Waals interaction and features temporary sequestration, whereas the CAD traps PS through strong chemical binding between the PS molecules and carbon surface featuring long-term sequestration, as schematically illustrated by Fig. 1. It is indicated that the PAB is able to increase the specific capacity of sulphur but fails to retain stable capacity because the weak absorption cannot effectively prevent out-diffusion of the negatively charged PS anions. In contrast, the CAD not only

increases the specific capacity but also stabilizes the capacity retention due to the strong sulphur sequestration.

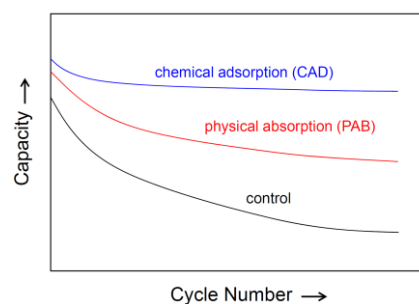


Fig. 1 Schematic comparison of physical absorption (PAB) and chemical adsorption (CAD) in improving the cycling performance of Li/S batteries.

The PAB is affected mainly by the physical properties of carbon such as the pore structure and porosity. In the past years, researches on the S-C composites have been overwhelmingly focused on the PAB strategy based on varieties of nanostructured porous carbon materials, which the readers may refer to several review articles.<sup>2-4-7</sup> In contrast, the CAD is much more complicated, which is affected not only by the electronic deficiency and hydrophilicity of carbon surface but also by the type and content of the surface functional groups. A single adsorption system may involve one or more types of chemical interactions. Since surface functional groups are merely the form of heteroatom (HA) existence with carbon, this review highlights the syntheses of HA-doped carbons and their CAD mechanism and applications in Li/S batteries with focus on oxygen, sulphur, nitrogen and their mixtures.

## 2. Synthesis and basic properties of HA-doped carbons

The scope of this review is limited to oxygen, sulphur, nitrogen and their mixtures. These HAs are typically presented in the form of functional groups, which are briefly summarized in Table 1. In the process of preparing S-C composites, some functional groups are thermally eliminated, or substituted/reduced by elemental sulphur to form so-called sulphurized carbon (SC) that together with the remaining HAs affects the CAD of carbon. There are two general approaches for the synthesis of HA-doped carbons: (1) the treatment of commercial or synthetic carbons with HA source and (2) the pyrolysis of HA-containing precursors. The former features the HAs doped on the surface of carbon with low HA content (typically not higher than 5 wt.%), and the latter features the HAs doped throughout the carbon bulk with high HA content up to more than 20 wt.%, for example 21.6 wt.% N for a N-doped carbon prepared by carbonizing N-containing ionic liquids.<sup>9</sup> Introduction of HAs into carbon changes the electronic distribution of the carbon conductive networks. The electronic conductivity of carbon will be dramatically declined when the content of HAs exceeds a certain level. Therefore, the conductivity and doping dose must be balanced when one designs HA-doped carbons for use in the Li/S batteries. Since the CAD occurs on the solution-carbon interface, only those HAs doped on the carbon surface are responsible for the sulphur sequestration. Therefore, the capacity and ability of CAD are determined mainly by the concentration and type of HAs on the carbon surface, other than the total HA content in the carbon bulk.

**Table 1** Typical forms of the functional groups for various heteroatoms

Heteroatom	Typical functional group with carbon
O	-OH, >O, >C=O, -C(=O)O-, -COOH
S	-S <sub>n</sub> H, -S <sub>n</sub> -, >C=S, -C(=S)S <sub>n</sub> -, -C(=S)S <sub>n</sub> H, -SO <sub>3</sub> H, -S(=O) <sub>2</sub> O-
N	-NH <sub>2</sub> , >NH, >N-, =N-, >N<, -N=O, -NO <sub>2</sub>

To be used in Li/S batteries, the HA-doped carbons can be either mixed with sulphur to form a S-C composite<sup>4, 5</sup> or coated as a PS-blocking layer onto the surface of sulphur cathodes<sup>2, 10</sup> or onto the separator facing the cathode.<sup>11, 12</sup> The S-C composites are prepared mostly through the sulphur melt diffusion method near the sulphur's critical temperature (159.4 °C) at which sulphur melt has the lowest viscosity for diffusing into the pores of carbon.<sup>13</sup> At such temperatures, in fact, significant amounts of the HAs and their functional groups will be thermally eliminated or substituted by sulphur to form SCs.<sup>14</sup> Therefore, small amounts of S-C covalent bonds are an important characteristic of the S-C composites with the HA-doped carbon.

### 3. Heteroatom-doped carbons

#### 3.1. Oxygen-doped carbons (ODC)

Oxygens in carbon are present in forms of hydroxyl (-OH), epoxy (>O), ketone (>C=O), ester (-C(=O)O-), and carboxylic acid (-COOH), which can be introduced by mild oxidation of carbons or pyrolysis of oxygen-containing precursors. The mild oxidation can be realized through a solid-gas reaction at high temperatures,<sup>15, 16</sup> or through a solid-liquid reaction at moderate temperatures.<sup>17</sup> The oxygen source may be water or CO<sub>2</sub> for the high temperature solid-gas reaction, and other relatively strong oxidizing agents such as H<sub>2</sub>O<sub>2</sub>, KMnO<sub>4</sub>, Na<sub>2</sub>S<sub>2</sub>O<sub>8</sub> and HNO<sub>3</sub> for the moderate

temperature solid-liquid reaction. For the pyrolysis approach, all organic compounds, natural or synthetic polymers can be used as the carbon precursor as long as they contain oxygen. At the temperatures of preparing S-C composites, the oxygen and oxygen-functionalized groups are easily eliminated, substituted, or reduced by sulphur to form S-C and S-O bonds. Therefore, the preparation of the S-C composites inevitably results in considerable reduction in the oxygen content, and the S-C and S-O bonds are typically characteristic of the S-C composites.<sup>15, 18, 19</sup> The role of the doped oxygen in enhancing the sulphur sequestration varies with the type of carbon-oxygen bonds in the ODC, which are highlighted below.

Due to the high surface area and high oxygen concentration of graphene oxide (GO), the two-dimensional structured GO was first proposed to anchor PS by Ji et al<sup>20</sup> who prepared a S-GO composite by first depositing sulphur onto GO via a solution method and then heating the mixture at 155 °C for 12 h. In this process, the >C=O bonds in the GO are reduced by sulphur and sulphur itself is oxidized to form sulphur-oxygen bonds while the epoxy and hydroxyl oxygens are substituted by sulphur to form C-S bonds. Therefore, resulting S-GO composites contain significant amounts of S-O and C-S bonds as identified by the K-edge X-ray absorption spectroscopy (XAS) spectra,<sup>18, 20</sup> which contribute to the sulphur sequestration by serving as a bridge to covalently immobilize sulphur species on the carbon surface. As a result, a Li/S cell with the S-GO composite exhibited a reversible capacity of 950-1400 mAh/g and cycled stably at 0.1C for more than 50 cycles.<sup>20</sup> This concept has been further studied and better understood by using either GO or reduced-GO (rGO) as the starting material.<sup>18, 19, 21, 22</sup> Owing to the reduction by sulphur, the ultimate S-C composites prepared from the GO and rGO turn out to have very similar chemistry. Beside the covalent S-O and C-S bonds, there are strong evidences for the >O<sup>-</sup>Li<sup>+</sup> binding between the epoxy oxygen and PS cluster.<sup>19</sup> Using first-principle molecular dynamics simulations and density functional theory (DFT) calculations, Wang et al<sup>23</sup> showed that the oxygens on graphene basal plane have adsorption energies of 1.1~1.5 eV with the Li<sub>2</sub>S<sub>8</sub> cluster, providing an excellent theoretical support for the enhancement of CAD by the oxygen HAs. A similar enhancement was reported by Yan et al<sup>24</sup> who treated carbon nanotubes (CNT) with a HNO<sub>3</sub>-H<sub>2</sub>SO<sub>4</sub> mixed acid and H<sub>2</sub>O<sub>2</sub>, respectively, and then loaded sulphur at 300 °C for 5 h. The S-O and C-S bonds are formed in the S-CNT composite as suggested by two new absorption bands at 1050 cm<sup>-1</sup> and 925 cm<sup>-1</sup>, respectively, in Fourier transform infrared (FTIR) spectroscopy. As a result, the S-CNT composite with a sulphur content of 68 wt.% showed an initial capacity of 1180 mAh/g and remained 799 mAh/g after 300 cycles at 0.25C. It should be noted that although detected spectroscopically, the S-O single bond is thermodynamically unstable with a trend being oxidized to more stable S=O double bond or broken into S· and O· radicals. The S-O single bond can be rarely found from small organic compounds except for those contained in the -SO<sub>3</sub>R groups (R=H, metal ion, or alkyl groups). Therefore, the contribution of the S-O bond to the sulphur sequestration may be very limited.

Mild oxidation of carbons is a facile and viable method for doping of oxygen into carbon. As an example, Xiao et al<sup>15</sup> treated porous CNTs with a water steam at 850 °C and then prepared a S-

C composite by mixing the treated carbon with sulphur and heating at 160 °C for 12 h and at 180 °C for another 12 h. High-resolution X-ray photoelectron spectroscopy (XPS) spectra of the resultant S-C composite show distinct characteristics of the S–O and C–S bonds. As a result, a Li/S cell with such a cathode material exhibited an initial capacity of 1165 mAh/g and remained 792 mAh/g after 200 cycles at 0.2C even when the sulphur content in the S-C composite reached as high as 89 wt.%. The XPS analyses verify that the excellent capacity and capacity retention are due to the enhanced CAD of carbon surface to sulphur species via the C–S and S–O bonds. However, discrepant results were reported by Li et al<sup>16</sup> who introduced oxygens into carbon by treating carbon with CO<sub>2</sub> at 1050 °C for several minutes and prepared a S-C composite by heating the sulphur-carbon mixture at 150 °C for 9 h and at 300 °C for additional 3 h. The cathode made by such a composite showed inferior performance, which these authors attributed to the reduced conductivity and possible side reactions occurring between sulphur and surface oxygens.

Provided that the oxygen-functionalized groups remain in the S-C composites, the  $>C=O\cdots Li(S_nLi)$ ,  $>O\cdots Li(S_nLi)$ , and  $Li_2S_n\cdots HO-$  bindings are possible to exist between the ODC and polysulphide species. The ab initio simulations on several common binders of the sulphur cathode by Sel et al<sup>25</sup> reveal that strong  $>C=O\cdots Li(S_nLi)$  binding exists between the double-bonded oxygens in the carbonyl groups and the Li<sup>+</sup> ions in Li<sub>2</sub>S and PS molecules with typical binding energies in a range of 1.20–1.26 eV. Based on this finding, Park et al<sup>26</sup> made significant improvement on the sulphur sequestration by coating CNTs with an ester-based polymer. The  $>O\cdots Li(S_nLi)$  binding was suggested by the DTF calculations, indicating that the epoxide and hydroxyl oxygens on graphene surface do not bind neutral S<sub>3</sub> cluster, instead they increase the binding between the graphene and negatively charged S<sub>3</sub><sup>-</sup> and S<sub>3</sub><sup>2-</sup> clusters indirectly through the  $O\cdots Li^+$  complexing bond as the binding bridge.<sup>19</sup> Sulphur sequestration by the  $Li_2S_n\cdots HO-$  hydrogen-bond was first proposed and experimentally verified by Zhang et al<sup>27</sup> who coated a gelable poly(acrylic acid) polymer onto the surface of a conventional sulphur cathode and observed a significant reduction in the out-diffusion of PS. In addition to enhancing the CAD, the oxygen HAs are also shown to improve the hydrophilicity of the carbon surface and facilitate the electrochemical redox of PS species on the carbon surface. The former improves the distribution of PS species and liquid electrolyte on the cathode, and the latter facilitates the deposition of insoluble sulphur reduction products (Li<sub>2</sub>S<sub>2</sub> and Li<sub>2</sub>S) in discharge.<sup>28, 29</sup>

Based on the above results, the roles of ODC in enhancing the sulphur sequestration can be summarized as: (1) covalently immobilizing PS anions onto carbon surfaces via S–C and S–O covalent bonds,<sup>15, 30</sup> (2) complexing PS molecules with carbon surfaces indirectly through  $>O\cdots Li^+$  and  $>C=O\cdots Li^+(S_nLi)^-$  bindings,<sup>23, 25</sup> (3) forming  $Li_2S_n\cdots HO-$  hydrogen-bond between the PS anion and –OH group,<sup>27</sup> and (4) increasing the hydrophilicity of carbon surfaces to facilitate the redox of sulphur species and the deposition of Li<sub>2</sub>S<sub>2</sub> and Li<sub>2</sub>S.<sup>28, 29</sup> The CAD in a single system may involve one or more of the chemical interactions listed above, depending on the type and concentration of the oxygen-functionalized groups on the surface of the ODC.

### 3.2. Sulphur-doped carbons (SDC)

SDC are typically made through three approaches: (1) sulphurizing of commercial or synthetic carbons with a sulphur source, (2) pyrolyzing of sulphur-containing precursors, and (3) heating of mixtures consisting of a carbon precursor and a sulphur source.<sup>31</sup> In these approaches, the sulphurization is based on reactions of surface functional groups on carbon with a sulphur source, in which the surface functional groups may be any species that can be thermally eliminated or substituted by sulphur such as C–H, –OH,  $>C=O$ ,  $-C(=O)OH$  and  $>C=C<$ . The sulphur source and precursor may be any type of compounds containing sulphur, such as elemental sulphur, H<sub>2</sub>S, SO<sub>2</sub>, CS<sub>2</sub>, sulphur-containing organic compounds and polymers. Of particular interest are sulphur-containing precursors in which the covalent C–S bonds are already present, providing a facile approach for making the SDC with relatively high sulphur content. In the SDC, sulphurs are present in multiple forms of functional groups, such as  $-S_nH$ ,  $-S_n-$ ,  $>C=S$ ,  $-C(=S)S_n-$ ,  $-C(=S)S_nH$ ,  $-S(=O)_2OH$ ,  $-S(=O)_2O-$ . However, these functional groups are eventually converted to the most stable monosulphur ( $-S-$ ) through the elimination or carbothermal reaction at elevated temperatures. With an increase in the sulphur content, two or more sulphur atoms tend to be combined into short polysulphide chains ( $-S_n-$ ) to form SC, which have long been studied as the efficient sorbent for heavy metal ion removal in environmental pollution treatment<sup>32</sup> and as a catalyst or catalyst support.<sup>31</sup> The temperature and pressure are two major factors affecting the sulphur content and the length of the polysulphide chains. In general, high temperature leads to short polysulphide chain and low sulphur content.<sup>33, 34</sup> As such, the SDC are one of the SC materials with low sulphur content and short polysulphide chain. Based on the results of elemental analysis and thermogravimetric analysis (TGA), a calculation on the SC made by heating a 1:4 (wt.) mixture of polyacrylonitrile and sulphur at 300 °C for 4 h shows that sulphurs are present in the form of short polysulphide chains with an averaged n value of 3.37 in the  $-S_n-$  chains even if the sulphur content reaches as high as 49.1 wt.%.<sup>35</sup> Since the SCs themselves are a class of high capacity cathode materials, previous efforts on the subject have been centred on the SCs with the sulphur content up to 50 wt.%.<sup>14</sup>

Since sulphurs in the SCs are covalently bound to carbon, they are neither removed by the conventional thermal vaporization near the sulphur's melting point (293 °C) nor extracted out by the solvent such as CS<sub>2</sub>, toluene, and electrolyte solvents.<sup>14</sup> Therefore, the redox of sulphur species in a Li/SC cell can only occur on the solid-solid two-phase interface (i.e. the SC and Li<sub>2</sub>S phases), leading to unique electrochemical behaviours compared with the conventional S-C composites, as illustrated in Fig. 2. Firstly, the Li/SC cell shows only a slightly sloping discharge voltage plateau at ~1.8 V due to the single solid-solid phase transition (Fig. 2a); Secondly, the first discharge of Li/SC cell suffers significant voltage hysteresis and irreversible capacity loss due to the large grain boundary resistance (GBR) of fresh SC particles and irreversible formation of solid electrolyte interphase (SEI) on the SC surface (Fig. 2a); Thirdly, the Li/SC cell prefers a carbonate-based electrolyte due to the insolubility of SC and its reduction intermediates/products, which substantially mitigates the reactivity of sulphur species with carbonate solvents (Fig. 2b). Other unique features of the Li/SC cells are near 100% coulombic efficiency, extremely low self-discharge, and excellent safety.<sup>14</sup>



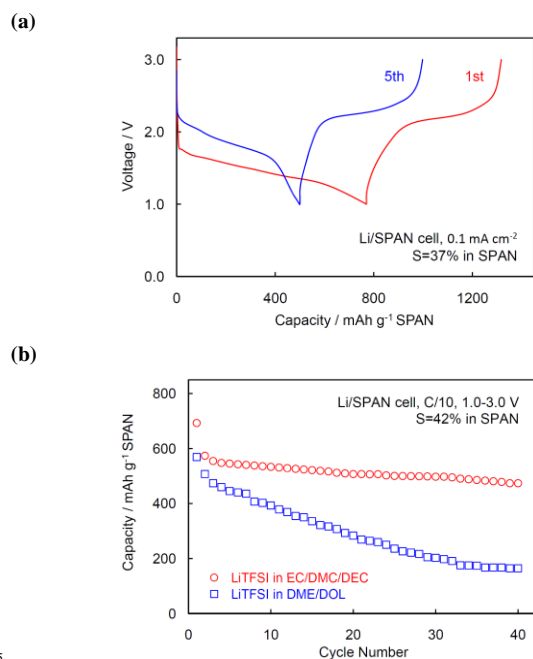


**Fig. 2** (a) Voltage profile and (b) electrolyte preference of the Li/SC cells. The figure is reprinted from ref. <sup>35</sup>, an open access without Copyright.

The SDC sequester soluble PS through sulphur-sulphur chemical interactions as indicated by eqn. 1 and eqn. 2, and the sequestering ability increases with a decrease in the length of polysulphide chains (i.e., the  $n$  value in the  $-S_n-$  chain). In solutions, it is possible for sulphur to covalently insert into the short  $-S_n-$  chains, forming longer chains, as indicated by eqn. 3.



The S-C composites with the SDC share many similarities with the SC materials, and hence the SC materials can be used to understand the role of the S-doped carbons in sulphur sequestration.

Synthetic carbons contain more or less surface functional groups. This feature has been widely adopted to produce the SC materials in large scale. In this effort, Chang<sup>36</sup> synthesized three SCs with the sulphur content of 24.8, 26.0, and 38.1%, respectively, by reacting carbon with  $SO_2$  at 600 °C for several hours, and showed that the Li/SC cells had a ~1.7 V discharge voltage plateau with a 96% sulphur utilization. A similar concept was reported by Kim et al<sup>37</sup> who heated a 1:5 (wt.) mixture of mesoporous hard carbon spheres and sulphur at 150 °C for 7 h and held the mixture at 300 °C for another 2 h. They observed that the stable SC could be formed only when the sulphur content was not more than 20 wt.%, beyond which extra sulphurs combine into elemental sulphur. On the other hand, based on the carbothermal

reaction of carbon, Ning et al<sup>38</sup> synthesized a SDC with the sulphur content up to 26.8 wt.% by reacting  $MgSO_4$  as the solid sulphur source with carbon at 700 °C for 30 minutes. They found that S-doping considerably enhanced the coulombic efficiency in the initial SEI formation of carbon anode material. In the same principle, Li et al<sup>39</sup> prepared a pre-lithiated SC by reacting  $Li_2SO_4$  and graphene nanoplatelet aggregates as indicated by eqn. 4, and found that the obtained product had excellent electrochemical behaviour in the Li/S batteries.



While numerous organic sulphides, sulphones, sulphonic acids, and thiophene-based compounds/polymers are available for the precursors of the SDC,<sup>31</sup> natural gas, liquefied natural gas and sulphurized rubbers (e.g. wasted tires) provide a vast resource of cheap and abundant precursors for large-scale production of the SDC by the pyrolysis of S-containing precursors. Owing to the limited sulphur content in these precursors and the inevitable loss of small S-containing molecular moieties in the pyrolysis, the sulphur contents in such-obtained SDC generally do not exceed 5 wt.%. Though such materials have been widely used for the removal of heavy metal ions in the environmental pollution treatment, there are no publications available for their applications in the Li/S batteries.

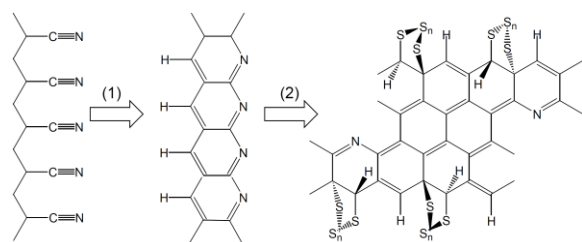
Heating of the mixture of a carbon precursor (preferably a non-volatile polymer) and elemental sulphur provides a facile approach for the preparation of SC materials with high sulphur content. In heating, elemental sulphur not only serves as the sulphur source but also acts as the dehydrogenator to promote the generation of  $>C=C<$  double bonds and resultant vulcanization. It was reported that sulphurized polyethylene could be made simply by heating a mixture of polyethylene (PE) and sulphur at 160-365 °C.<sup>40</sup> This process typically produced sulphurized polyethylene with a sulphur content of 20-80 wt.% and a conductivity of  $4.4 \times 10^{-14} \sim 2.0 \times 10^{-9}$  S/cm, depending on the PE/S ratio, heating temperature and time. Interestingly, the conductivity increases to a range of  $2.0 \times 10^{-7} \sim 4.9 \times 10^{-6}$  S/cm when doped with iodine, indicating that the well-conjugated  $>C=C<$  double bonds are present in the sulphurized polyethylene.

Sulphurization of polyacrylonitrile (PAN) was first reported by Wang et al<sup>41</sup> who heated a mixture of PAN and sulphur at 280 to 300 °C in argon for 6 h, and followed by intensive investigation to optimize the sulphurization conditions and understand the electrochemistry of sulphurized polyacrylonitrile (SPAN).<sup>42-44</sup> Though still poorly understood and debated, the PAN sulphurization can be generally described by Scheme 1. In heating, elemental sulphur dehydrogenates PAN to produce  $>C=C<$  double bonds by loss of small  $H_2S$  molecules and the  $-CN$  group promotes cyclization of conjugated six-member aromatic rings. Meanwhile, sulphur vulcanizes the resultant  $>C=C<$  double bonds to form C-S bonds, through which the short polysulphide chains are covalently bound to the cyclized, partially dehydrogenated, and ribbon-like PAN backbones.<sup>35, 45</sup>

Cite this: DOI: 10.1039/c0xx00000x

www.rsc.org/xxxxxx

Review

(1) Sulfur-assisted cyclization by release of H<sub>2</sub>S; (2) Vulcanization**Scheme 1** Reactions involved in the PAN sulphurization and possible chemical structure of SPAN.

Suitable temperature for the PAN sulphurization is in a range of 280 to 550 °C, which typically generates SPAN with a sulphur content of 30-55 wt.%. In general, high temperature leads to low sulphur content and short polysulphide chain with relatively high electronic conductivity, which corresponds to low specific capacity but stable capacity retention; low temperature can neither break down the S<sub>8</sub> ring into small S<sub>n</sub> molecules nor dehydrogenate polymer effectively, resulting in high sulphur content and long polysulphide chain with relatively low electronic conductivity, which corresponds to high specific capacity but fast capacity fading.<sup>46, 47</sup> Since the short polysulphide chains are covalently bound to the polymer backbone, the SPANs are thermally stable until 450 °C and do not form soluble PS in discharge, exhibiting very stable capacity retention, extremely low self-discharge, and excellent safety.<sup>14</sup> By optimizing the PAN/S ratio, sulphurization temperature and time, Wang et al<sup>43</sup> synthesized a SPAN with 42 wt.% S, showing that the Li/SC cell had a specific capacity of 811 mAh/g with respect to the mass of entire SPAN in the second discharge and stabilized 795 mAh/g after 50 cycles. These numbers are even higher than the theoretical capacity (1675 mAh/g) of elemental sulphur if normalized to the mass of active sulphur in the SPAN, because of the extra contribution of conjugated SPAN polymeric backbones to the overall capacity.<sup>14, 35, 45</sup> Inspired by the knowledge of rubber vulcanization, on the other hand, Chen et al<sup>48</sup> added ~5 wt.% 2-mercaptobenzothiazole (a common vulcanization accelerator for rubber vulcanization) into a 1:1 PAN/S mixture, which led the SPAN to a ~8 wt.% increase in the sulphur content and a ~120 mAh/g increase in the specific capacity compared with the control. This finding reveals that the vulcanization accelerator effectively enhances the efficiency of sulphurization, offering a facile method for the preparation of SPAN and other SCs.

On the other hand, See et al<sup>49</sup> modified mesoporous carbon by in-situ polymerizing thiophene onto carbon surface and then pyrolyzing at 800 °C in a 5% H<sub>2</sub> flow for 4 h. The XPS analysis verified that sulphurs in SDC were covalently bound to carbon, and a cell cycling test showed that a 5.5 wt.% S doping led to as high as a 50% increase in the capacity of S-C composite with much stable retention, as compared with the pristine carbon, although they found these sulphurs did not provide any capacities. Suggested by the relatively low heats observed when PS species

were titrated into SDC, they considered that the achieved improvement in sulphur sequestration was due to the enhanced affinity between the strongly polar PS anions and non-polar carbon surface as a result of the S-doping converting carbon surface from hydrophobic to hydrophilic property. In fact, this explanation is in principle not contradictory with eqn. 1, predicting that the S...S complex binding between the PS anions and SDC contributes to the sulphur sequestration of SDC. In addition, it should be pointed out that the Li/S cells by See et al did not behave like a Li/SC battery, instead exhibited two distinct voltage plateaus at ~2.3 V and ~2 V, respectively, in the first discharge.<sup>49</sup> This is because (1) the S-C composite was prepared at relatively low temperature (155 °C for 2 h), which could not enable effective sulphurization, and (2) ethylmethyl sulfone was used as the electrolyte solvent, in which PS has high solubility.

In brief, the SDC sequester sulphur species through the C-S bonds that anchor short polysulphide anions to carbon via either S...S complex binding (eqn. 1) or S-S covalent binding (eqn. 2). In solutions, it is possible for sulphur to covalently insert into the short polysulphide chains in the SDC, forming longer polysulphide chains (eqn. 3). The sulphur content and the polysulphide chain length are two important factors determining the sequestering efficiency. When the sulphur content is low, the S-C composites with SDC behave in very similar manners as the SCs that show only a single discharge voltage plateau at ~1.8 V and prefer a carbonate-based electrolyte for cycling.

### 3.3 Nitrogen-doped carbons (NDC)

In order to distinguish nitrogen-rich compounds such as graphitic carbon nitride (C<sub>3</sub>N<sub>4</sub>), NDC are referred as to these carbons with the N/C atomic ratio less than 1. The NDC are prepared either by post-treatment of carbons with a nitrogen source such as NH<sub>3</sub> and CH<sub>3</sub>CN or by carbonization of nitrogen-containing precursors.<sup>9</sup> The post-treatment generally dopes nitrogen on the surface with the nitrogen content lower than 5 wt.% whereas the carbonization dopes nitrogen throughout the bulk with the nitrogen content up to more than 20 wt.%. The nitrogen content in NDC greatly depends on the precursor and preparation conditions with a trend that high reaction temperature leads to low nitrogen content.<sup>9, 50</sup> In order to obtain high nitrogen content, non-volatile ionic liquids and polymers are preferable precursors. However, the upper limits of the nitrogen content are 14.32 wt.% for those made at 1000 °C and 21.66 wt.% for those made at 900 °C, irrespective of the precursor or preparation conditions.<sup>9</sup>

Identified by three distinguishable peaks in binding energy range of 398~404 eV in the high resolution XPS spectra,<sup>51-53</sup> nitrogens in NDC are present in three main forms of pyridinic N, pyrrolic N, and quaternary N, as indicated in Fig. 3. The ab initio calculations indicate that the first two types of nitrogens are more effective in forming Li<sub>n</sub>Li<sup>+</sup>...N binding and dominate the sequestration of Li<sub>2</sub>S<sub>n</sub>.<sup>52</sup> Other nitrogen-functionalized groups such as -NH<sub>2</sub>, -CN, -N=O and -NO<sub>2</sub> groups are rarely present because -NH<sub>2</sub> is either eliminated in pyrolysis or substituted by sulphur in

the process of making S-C composites;  $-\text{CN}$  is easily eliminated or converted to more stable pyridinic or pyrrolic nitrogens by forming conjugated aromatic rings in pyrolysis;  $-\text{N}=\text{O}$  and  $-\text{NO}_2$  are carbothermally reduced in pyrolysis. Sulphur sequestration of NDC is mainly through the chemical binding between the  $\text{Li}^+$  ion in  $\text{Li}_2\text{S}_n$  and the strong electron-donating lone-pair electrons in nitrogen, namely the  $\text{LiS}_n\text{Li}^+\cdots\text{N}$  binding. The similar principle is well-known in solution chemistry and has long been used for the syntheses of polysulphide clusters of alkaline earth metals and transition metals, in which N-containing solvents were frequently used to promote the dissolution of polysulphide clusters through strong solvation between the metal ion and the lone-pair electrons of nitrogen.<sup>54-56</sup> Beside the  $\text{LiS}_n\text{Li}^+\cdots\text{N}$  binding, the C-S bond makes additional contribution to the sulphur sequestration because the synthetic carbons contain more or less hydrogens that are dehydrogenated by sulphur and subsequently vulcanized to form C-S bond in the process of making S-C composites.

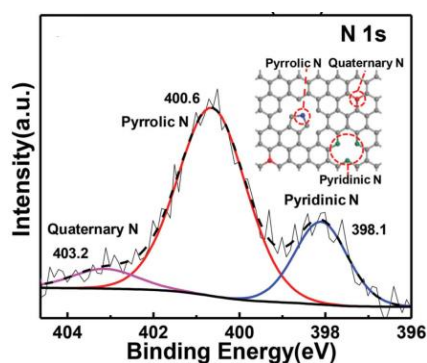


**Fig. 3** XPS spectrum of NDC and three main forms of nitrogens in NDC. The figure is reprinted with permission from ref.<sup>53</sup>. Copyright (2015) John Wiley and Sons.

Using the post-treatment method, Qiu et al<sup>52</sup> prepared N-doped graphene by treating GO sheets in a  $\text{NH}_3$  atmosphere at  $750^\circ\text{C}$  for 30 minutes. It was shown that the treatment not only reduced GO but also introduced nitrogens into the graphene sheets, resulting in N-doped graphene with an N/C atomic ratio of  $\sim 3.9\%$ . The cathode with a 60 wt.% S versus the overall electrode delivered initial capacities of  $\sim 1167$  mAh/g at 0.2C and  $\sim 802$  mAh/g at 2C, and cycled for 2000 cycles with an averaged capacity fading rate as low as 0.028% per cycle and an averaged coulombic efficiency of above 97%. The XPS analysis and ab initio calculation indicate that the excellent performances are due to the strong  $\text{LiS}_n\text{Li}^+\cdots\text{N}$  binding that effectively hinders the dissolved PS from diffusing out of the cathode. Using the same principle, Li et al<sup>16</sup> treated a commercial carbon black with  $\text{NH}_3$  at  $1050^\circ\text{C}$  for 3-5 minutes, which led to a NDC with 1.5 wt.% N. Using such an NDC, a S-C composite with a 60 wt.% S was prepared and shown to have significantly improved capacity, capacity retention and rate capability compared with the control. In particular, the composite delivered a capacity of about 1490 mAh/g in the first discharge and retained 1020 mAh/g after 40 cycles with a coulombic efficiency of 93%. The XPS analysis indicates that the defect sites of NDC are favourable for the deposition of discharge products, leading to high utilization and reversibility of sulphur cathodes. This observation agrees with the fact that the N atoms chemically adsorb PS molecules through the  $\text{LiS}_n\text{Li}^+\cdots\text{N}$  binding and consequently facilitate the electrochemical redox of PS on the

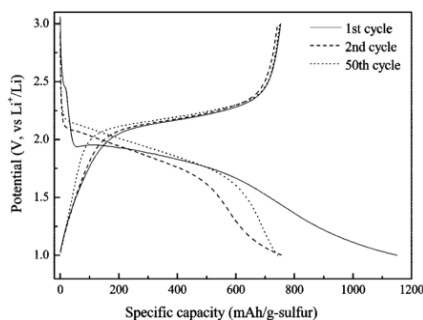
carbon surface.

Carbonization of N-containing precursors has been one of the most studied approaches for the preparation of NDC. In this practice, Xu et al<sup>57</sup> synthesized a NDC by pyrolyzing a polydopamine at  $800^\circ\text{C}$  for 1 h, and used it to prepare a S-DNC composite. Results showed that the composite retained a reversible capacity of  $\sim 605$  mAh/g after 500 cycles at 2C with a low capacity fading rate of 0.030% per cycle. In addition to the highly porous structure of NDC, the strong chemical interactions of the electron-donating N and O atoms with the  $\text{Li}^+$  ions in PS molecules are responsible for this excellent cyclability. Aiming to enhance the efficiency of sulphur sequestration, Sun et al<sup>58</sup> developed a colloidal silica assisted sol-gel process for the preparation of mesoporous NDCs. In their process, a mixture of phenol, melamine and formaldehyde was condensed in a solution containing  $\text{SiO}_2$  sol. The resulting polymer resin was dried and carbonized at  $800^\circ\text{C}$  for 3 h, followed by etching  $\text{SiO}_2$  away to generate a mesoporous structure. They found that N-doping assisted mesoporous carbon to sequester sulphur through enhanced surface interactions between the basic nitrogen functionalities and polysulphide species, but meanwhile adversely affected the electronic conductivity of the carbon matrix. Only when the nitrogen content is in a range of 4-8 wt.%, the NDC are able to improve the performance of Li/S batteries. An optimal nitrogen content was determined to be 8.1 wt.%, which resulted in the S-C composite demonstrating a reversible capacity of 758

75 mAh/g at 0.2C and 620 mAh/g at 1C after 100 cycles. Conducting polymers such as polyaniline and polypyrrole have been proven to be excellent precursors for NDC with novel pore structure because of their flexibility and easiness to be synthesized into desirable nanopore structures. In this effort, Xiao et al<sup>59</sup> synthesized polyaniline nanotubes, followed by treating them with sulphur at  $280^\circ\text{C}$  to obtain an S-NDC composite. As a result of the in-situ vulcanization, the obtained composite is of three-dimensional structure with covalently crosslinked polymeric frameworks that provide strongly physical and chemical sequestration to sulphur. After tens of activation cycles, which was due to the poor penetration of liquid electrolyte into the nanostructured pores, the S-NDC composite exhibited superior cycling stability and rate capability with an initial capacity of 755 mAh/g at 0.1C, which stabilized 837 mAh/g after 100 cycles. When cycled at 1C, the cell was able to retain a capacity of 432 mAh/g with a coulombic efficiency of over 90% even after 500 cycles. The observed improvement is attributed to not only the novel nanostructured pores but also the enhanced chemical binding between the electron-donating N atoms and polysulphide species. Pyrolyzed PAN is of particular interest in understanding of the sulphur sequestration mechanism of NDC. In order to confirm the  $\text{LiS}_n\text{Li}^+\cdots\text{N}$  interactions, two composites of the pyrolyzed PAN with elemental sulphur and lithium polysulphide ( $\text{Li}_2\text{S}_3$ ), respectively, were prepared by the procedures described in Table 2 and compared in Fig. 4. It can be observed from Fig. 4a<sup>60</sup> that the S-NDC composite without  $\text{Li}^+$  ions in its initial composition shows only a single discharge voltage plateau at  $\sim 1.8$  V, indicative of a SC in which the sulphur species are sequestered through the C-S bond formed in the process of making the S-NDC composite through the vulcanization of  $>\text{C}=\text{C}<$  double bonds and the substitution of sulphur for remaining hydrogens and removable

nitrogen-functionalized groups such as  $-\text{NH}_2$ . In contrast, the  $\text{Li}_2\text{S}_3$ -NDC composite with  $\text{Li}^+$  ions in its initial composition exhibits two discharge voltage plateaus at  $\sim 2.3$  V and  $\sim 2$  V, as shown in Fig. 4b,<sup>61</sup> with significantly improved capacity and capacity retention compared with the conventional  $\text{Li}_2\text{S}_3$ -C composite. Remarkable difference in the cells' voltage profile between the S-NDC and  $\text{Li}_2\text{S}_3$ -NDC composites strongly supports the role of  $\text{LiS}_n\text{Li}^+\cdots\text{N}$  binding in sulphur sequestration.

10 (a)



(b)

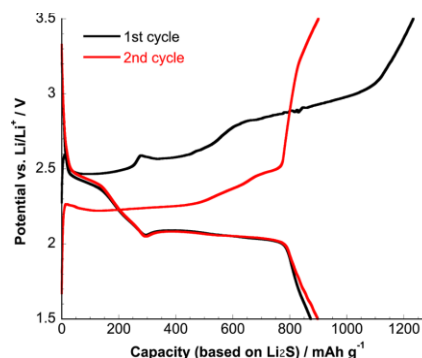


**Fig. 4** Voltage profile of (a) S-NDC composite and (b)  $\text{Li}_2\text{S}_3$ -NDC composite. The figures are reprinted with permission from refs. <sup>60</sup> and <sup>61</sup>. Copyright (2009 and 2013) American Chemical Society.

**Table 2** Comparison of S-NDC and  $\text{Li}_2\text{S}_3$ -NDC composites

	S-NDC composite	$\text{Li}_2\text{S}_3$ -NDC composite
Preparation	PAN and $\text{Na}_2\text{CO}_3$ were mixed using DMF solvent, followed by pyrolyzing at $750$ °C for 2 h; A composite with 57 wt.% S was prepared by heating a S-NDC mixture at $300$ °C for 3 h	PAN was dissolved into a $\text{Li}_2\text{S}_3$ DMF solution, followed by drying and pyrolyzing at $300$ °C for 2h and at $600$ °C for another 30 min.
Electrolyte	1 M $\text{LiPF}_6$ 1:4:5 (vol.) PC/EC/DEC	1 M LiTFSI 1:1 (vol.) TG/PYR14TFSI
Results	Significant capacity loss in the 1st discharge; A single discharge voltage plateau at $\sim 1.8$ V	Significant capacity loss in the 1st charge; Two discharge voltage plateaus at $\sim 2.3$ V and $\sim 2$ V, respectively
Comment	Behave as a sulphurized carbon; Sequester sulphur via C-S bond	Behave as a normal Li/S cell; Sequester sulphur via $\text{LiS}_n\text{Li}^+\cdots\text{N}$ binding
Reference	<sup>60</sup>	<sup>61</sup>

Note: DMF=N, N-dimethyl formamide, PC=propylene carbonate, EC=ethylene carbonate, DEC=diethylene carbonate, LiTFSI=lithium bis(trifluoromethanesulfonyl)imide, TG=tetraethylene glycol dimethyl ether, and PYR14TFSI=N-methyl-(N-butyl) pyrrolidinium bis(trifluoromethanesulfonyl)imide.

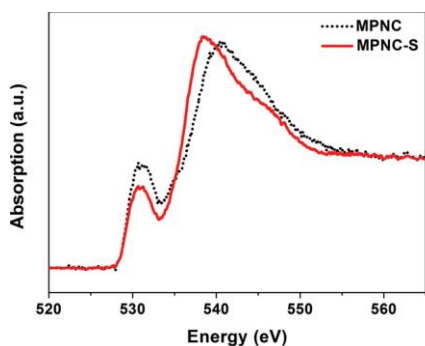
### 3.4. Multiple HA codoped carbons

As highlighted above, the oxygen, sulphur, and nitrogen HAs enhance the sulphur sequestration in different mechanisms. Thus, there is a need to know whether codoping of these HAs can lead to synergistic improvement on the sulphur sequestration. In this effort, Wang's group intensively investigated O, N-codoped mesoporous carbon that was synthesized by heating a mixture of poly(melamine-co-formaldehyde) resin as the carbon precursor and colloidal silica nanoparticles as the pore generator at  $900$  °C for 2 h, followed by removal of silica using hydrofluoric acid solution.<sup>62, 63</sup> The resultant mesoporous carbon, containing the oxygen- and nitrogen-functionalized groups, was mixed with sulphur and heated at  $155$  °C for 10 h to form a C-S nanocomposite. While obtaining much improved capacity and capacity retention, they analysed K-edge X-ray absorption near edge structure (XANES) spectra of the O, N and S atoms, finding that the C and N spectra were barely changed before and after sulphur loading because there were no  $\text{Li}^+$  ions in the C-S composite. This

observation coincides with the conclusion that the doped N atoms adsorb PS species through  $\text{Li}^+$  ions, namely the  $\text{LiS}_n\text{Li}^+\cdots\text{N}$  binding as reported elsewhere,<sup>51-53</sup> other than directly through the sulphur atoms. However, the O K-edge XANES spectrum was subject to considerable change after sulphur loading as shown in Fig. 5a, whereas the similar change was not observed from the counterpart carbon without N-doping. Therefore, these authors attributed the improved sulphur sequestration to the enhanced chemical adsorption between sulphur species and oxygen-functionalized groups on the carbon surface, which was promoted by the N-doping. Based on the DFT calculations, these authors proposed chemical adsorption of sulphur species through the O-S bonds, as schematically illustrated in Fig. 5b.<sup>63</sup> However, these authors did not explain how the  $-\text{OSO}_2-$  group and  $-\text{OSO}_3^-$  anion with the S valence of +6 were formed under the strongly reductive environment where the S-C composite was prepared.

(a)





(b)

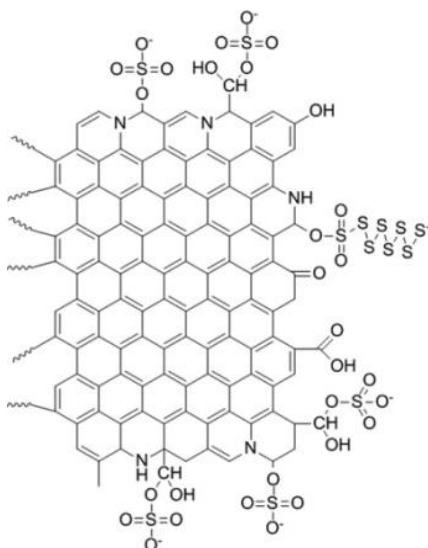


**Fig. 5** (a) Oxygen K-edge XANES spectra before and after sulphur loading,<sup>62</sup> (b) proposed chemical binding between sulphur species and oxygen-functionalized groups.<sup>63</sup> The figures are reprinted with permission from refs. <sup>62</sup> and <sup>63</sup>. Copyright (2014) John Wiley and Sons and Copyright (2014) American Chemical Society.

On the other hand, Zhou et al<sup>64</sup> investigated synergistic effect of N, S-codoping on the sulphur sequestration. They prepared N, S-codoped graphene sponge by the hydrothermal reaction of GO sponge and thiourea at 180 °C for 12 h, and compared it with the single S-doped and N-doped counterparts. The S 2p XPS spectrum of N, S-codoped graphene shows distinct binding energy peaks of S–O bond at 165.9 eV, S–S/S–C bonds at 164.9 and 163.7 eV; and the N 1s XPS spectrum shows peaks of quaternary N at 401.2 eV, pyrrolic N at 399.7 eV, and pyridinic N at 398.6 eV. Using graphene sponge as the cathode current collector and a 1.0 M Li<sub>2</sub>S<sub>6</sub> solution as the catholyte, Li/dissolved polysulphide cells were assembled and tested. A long-term cycling test indicated that N, S-codoping remarkably enhanced the specific capacity and rate capability compared with the single HA-doping in an order of N, S-codoped graphene >> N-doped graphene > S-doped graphene > O-doped graphene (i.e. rGO). In particular, the N, S-codoped graphene cell exhibited an initial capacity of 925 mAh/g and stabilized ~670 mAh/g after 200 cycles. The DFT calculations on several small model compounds reveal that the remarkable superiority is attributed to the synergistic enhancement of N, S-codoping in the chemical binding between the sulphur/nitrogen heteroatoms and lithium polysulphide/Li<sub>2</sub>S, which significantly reduces the loss of sulphur active material and consequently suppresses the redox shuttle effect.

## 4. Conclusions and outlook

Porous carbons sequester sulphur species through PAB and CAD. The PAB depends on the pore structure and porosity of carbons, whereas the CAD relies on the specific surface area and surface functional groups. The CAD not only sequesters sulphur species but also facilitates the redox and deposition of sulphur species on the carbon surface, leading to high specific capacity and stable capacity retention. The CAD capacity of HA-doped carbons to sulphur species increases with the concentration of HAs (i.e. the adsorbing sites), which on the other hand adversely affects the electronic conductivity of carbon matrix, leading to an optimal concentration for the performance of Li/S batteries. The oxygen, sulphur, and nitrogen HAs enhance the CAD by different mechanisms. Oxygen-functionalized groups are either removable or oxidative, which are easily eliminated or reacted with sulphur to form C–S bond in the process of preparing C–S composites. In addition to the C–S bonds that covalently anchor short polysulphide chains to carbon surface, remaining oxygens are also responsible for sulphur sequestration through the >C=O–Li<sup>+</sup>S<sub>n</sub>Li, >O–Li<sup>+</sup>S<sub>n</sub>Li, and –OH–Li<sup>+</sup>S<sub>n</sub>Li bindings. In the S-doped carbons, sulphurs are able to exist up to 50 wt.% in the form of short polysulphide (–S<sub>n</sub>–) chains, which are covalently bound to the surface or/and frameworks of carbon. Therefore, the S-doped carbons sequester sulphur mainly through the C–S bond. Nitrogen-functionalized groups are strongly bound to the graphitic plane in three main forms of pyridinic, pyrrolic, and quaternary nitrogens, among which the first two types of nitrogens are more effective in forming LiS<sub>n</sub>Li<sup>+</sup>–N binding via the N lone-pair electrons. Unless formed during the pyrolysis of the mixture of nitrogen-containing precursors and elemental sulphur, the C–S bonds are barely present in the N-doped carbons. Therefore, the N-doped carbons sequester sulphur mainly through the LiS<sub>n</sub>Li<sup>+</sup>–N binding, a similar principle of the metal ion solvation in solution chemistry. Since hydrogens inevitably exist in the synthetic carbons and sulphur is an excellent dehydrogenator, the process of preparing S–C composites near or above the sulphur's critical temperature (159.4 °C) results in the formation of more or less C–S bonds, which makes additional contribution to the sulphur sequestration. Codoping of two or more HAs may lead to synergistic enhancement in the sulphur sequestration, which could be a promising direction for future development of porous carbon materials to be used in practically viable Li/S batteries.

## 75 Acknowledgments

The author thanks Dr. C. Lundgren for her critical reading of the manuscript and valuable suggestions.

## Notes and references

- <sup>64</sup>Electrochemistry Branch, RDRL-SED-C, Sensors and Electron Devices Directorate, U.S. Army Research Laboratory, Adelphi, MD 20783-1138, USA. Fax: 1-301-394-0273; Tel: 1-301-394-0981; Email: shengshui.zhang.civ@mail.mil, or shengshui@gmail.com
1. S. S. Zhang, *J. Power Sources*, 2013, **231**, 153–162.
  2. A. Manthiram, Y. Fu, S. H. Chung, C. Zu and Y. S. Su, *Chem. Rev.*, 2014, **114**, 11751–11787.
  3. S. Urbonaitė, T. Poux and P. Novák, *Adv. Energy Mater.*, 2015, in press. DOI: 10.1002/aenm.201500118.

4. D. W. Wang, Q. Zeng, G. Zhou, L. Yin, F. Li, H. M. Cheng, I. R. Gentle and G. Q. M. Lu, *J. Mater. Chem. A*, 2013, **1**, 9382–9394.
5. Y. Yang, G. Zheng and Y. Cui, *Chem. Soc. Rev.*, 2013, **42**, 3018–3032.
6. S. Evers and L. F. Nazar, *Acc. Chem. Res.*, 2013, **46**, 1135–1143.
7. L. Ma, K. E. Hendrickson, S. Wei and L. A. Archer, *Nano Today*, 2015, **10**, 315–338.
8. J. Wang, Y. S. He and J. Yang, *Adv. Mater.*, 2015, **27**, 569–575.
9. S. Zhang, S. Tsuzuki, K. Ueno, K. Dokko and M. Watanabe, *Angew. Chem. Int. Ed.*, 2015, **54**, 1302–1306.
10. Q. Zeng, X. Leng, K. H. Wu, I. R. Gentle and D. W. Wang, *Carbon*, 2015, **93**, 611–619.
11. G. Zhou, L. Li, D. W. Wang, X. Y. Shan, S. Pei, F. Li and H. M. Cheng, *Adv. Mater.*, 2015, **27**, 641–647.
12. Z. Yunbo, M. Lixiao, N. Jing, X. Zhichang, H. Long, W. Bin and Z. Linjie, *2D Mater.*, 2015, **2**, 024013. doi:10.1088/2053-1583/2/2/024013
13. B. Meyer, *Chem. Rev.*, 1976, **76**, 367–388.
14. S. S. Zhang, *Front. Energy Res.*, 2013, **1**, 10. doi:10.3389/fenrg.2013.00010.
15. Z. Xiao, Z. Yang, H. Nie, Y. Lu, K. Yang and S. Huang, *J. Mater. Chem. A*, 2014, **2**, 8683–8689.
16. X. Li, X. Li, M. N. Banis, B. Wang, A. Lushington, X. Cui, R. Li, T. K. Sham and X. Sun, *J. Mater. Chem. A*, 2014, **2**, 12866–12872.
17. W. Zhou, S. Sasaki and A. Kawasaki, *Carbon*, 2014, **78**, 121–129.
18. L. Zhang, L. Ji, P. A. Glans, Y. Zhang, J. Zhu and J. Guo, *Phys. Chem. Chem. Phys.*, 2012, **14**, 13670–13675.
19. G. Zhou, L. C. Yin, D. W. Wang, L. Li, S. Pei, I. R. Gentle, F. Li and H. M. Cheng, *ACS Nano*, 2013, **7**, 5367–5375.
20. L. Ji, M. Rao, H. Zheng, L. Zhang, Y. Li, W. Duan, J. Guo, E. J. Cairns and Y. Zhang, *J. Am. Chem. Soc.*, 2011, **133**, 18522–18525.
21. J. W. Kim, J. D. Ocon, D. W. Park and J. Lee, *J. Energy Chem.*, 2013, **22**, 336–340.
22. X. Feng, M. K. Song, W. C. Stolte, D. Gardenghi, D. Zhang, X. Sun, J. Zhu, E. J. Cairns and J. Guo, *Phys. Chem. Chem. Phys.*, 2014, **16**, 16931–16940.
23. B. Wang, S. M. Alhassan and S. T. Pantelides, *Phys. Rev. Appl.*, 2014, **2**, 034004. DOI: 10.1103/PhysRevApplied.2.034004.
24. J. Yan, X. Liu, X. Wang and B. Li, *J. Mater. Chem. A*, 2015, **3**, 10127–10133.
25. Z. W. Seh, Q. Zhang, W. Li, G. Zheng, H. Yao and Y. Cui, *Chem. Sci.*, 2013, **4**, 3673–3677.
26. K. Park, J. H. Cho, J. H. Jang, B. C. Yu, A. T. De La Hoz, K. M. Miller, C. J. Ellison and J. B. Goodenough, *Energy Environ. Sci.*, 2015, **8**, 2389–2395.
27. S. S. Zhang, D. T. Tran and Z. Zhang, *J. Mater. Chem. A*, 2014, **2**, 18288–18292.
28. X. Feng, M. K. Song, W. C. Stolte, D. Gardenghi, D. Zhang, X. Sun, J. Zhu, E. J. Cairns and J. Guo, *Phys. Chem. Chem. Phys.*, 2014, **16**, 16931–16940.
29. J. H. Kim, K. Fu, J. Choi, S. Sun, J. Kim, L. Hu and U. Paik, *Chem. Commun.*, 2015, in press. DOI: 10.1039/C5CC04103A.
30. J. W. Kim, J. D. Ocon, D. W. Park and J. Lee, *J. Energy Chem.*, 2013, **22**, 336–340.
31. W. Kiciński, M. Szala and M. Bystrzejewski, *Carbon*, 2014, **68**, 1–32.
32. K. A. Krishnan and T. S. Anirudhan, *Ind. Eng. Chem. Res.*, 2002, **41**, 5085–5093.
33. J. A. Korpiel and R. D. Vidic, *Environ. Sci. Tech.*, 1997, **31**, 2319–2325.
34. Seekjoon Kwon and Radisav D. Vidic, *Environ. Eng. Sci.*, 2000, **17**, 303–313. doi:10.1089/ees.2000.17.303.
35. S. S. Zhang, *Energies*, 2014, **7**, 4588–4600. doi:10.3390/en7074588.
36. C. H. Chang, "Carbon-sulphur compounds as cathodes for lithium high energy secondary cells", in Proceedings of 29th Power Sources Conference (Pennington, NJ, The Electrochemical Society, Inc.), 1980, 208–211.
37. J. Kim, D. J. Lee, H. G. Jung, Y. K. Sun, J. Hassoun and B. Scrosati, *Adv. Funct. Mater.*, 2013, **23**, 1076–1080.
38. G. Ning, X. Ma, X. Zhu, Y. Cao, Y. Sun, C. Qi, Z. Fan, Y. Li, X. Zhang, X. Lan and J. Gao, *ACS Appl. Mater. Interfaces*, 2014, **6**, 15950–15958.
39. Z. Li, S. Zhang, C. Zhang, K. Ueno, T. Yasuda, R. Tatara, K. Dokko and M. Watanabe, *Nanoscale*, 2015, in press. DOI: 10.1039/C5NR03201F.
40. B. A. Trofimov, T. A. Skotheim, A. G. Mal'kina, L. V. Sokolyanskaya, G. F. Myachina, S. A. Korzhova, E. S. Stoyanov and I. P. Kovalev, *Russ. Chem. Bull.*, 2000, **49**, 863–869.
41. J. Wang, J. Yang, J. Xie and N. Xu, *Adv. Mater.*, 2002, **14**, 963–965.
42. X. He, Q. Shi, X. Zhou, C. Wan and C. Jiang, *Electrochim. Acta*, 2005, **51**, 1069–1075.
43. L. Wang, X. He, J. Li, J. Gao, J. Guo, C. Jiang and C. Wan, *J. Mater. Chem.*, 2012, **22**, 22077–22081.
44. L. Wang, X. He, J. Li, M. Chen, J. Gao and C. Jiang, *Electrochim. Acta*, 2012, **72**, 114–119.
45. J. Fanous, M. Wegner, J. Grimminger, Å. Andresen and M. R. Buchmeiser, *Chem. Mater.*, 2011, **23**, 5024–5028.
46. X. Yu, J. Xie, Y. Li, H. Huang, C. Lai and K. Wang, *J. Power Sources*, 2005, **146**, 335–339.
47. J. Fanous, M. Wegner, J. Grimminger, M. Rolff, M. B. M. Spera, M. Tenzer and M. R. Buchmeiser, *J. Mater. Chem.*, 2012, **22**, 23240–23245.
48. H. Chen, C. Wang, C. Hu, J. Zhang, S. Gao, W. Lu and L. Chen, *J. Mater. Chem. A*, 2015, **3**, 1392–1395.
49. K. A. See, Y. S. Jun, J. A. Gerbec, J. K. Sprafke, F. Wudl, G. D. Stucky and R. Seshadri, *ACS Appl. Mater. Interfaces*, 2014, **6**, 10908–10916.
50. J. P. Paraknowitsch, J. Zhang, D. Su, A. Thomas and M. Antonietti, *Adv. Mater.*, 2010, **22**, 87–92.
51. Y. Wang, Y. Shao, D. W. Matson, J. Li and Y. Lin, *ACS Nano*, 2010, **4**, 1790–1798.
52. Y. Qiu, W. Li, W. Zhao, G. Li, Y. Hou, M. Liu, L. Zhou, F. Ye, H. Li, Z. Wei, S. Yang, W. Duan, Y. Ye, J. Guo and Y. Zhang, *Nano Lett.*, 2014, **14**, 4821–4827.
53. G. Zhou, Y. Zhao and A. Manthiram, *Adv. Energy Mater.*, 2015, **5**, 1402263. DOI: 10.1002/aenm.201402263.
54. E. Ramli, T. B. Rauchfuss and C. L. Stern, *J. Am. Chem. Soc.*, 1990, **112**, 4043–4044.
55. S. Dev, E. Ramli, T. B. Rauchfuss and S. R. Wilson, *Inorg. Chem.*, 1991, **30**, 2514–2519.
56. A. K. Verma, T. B. Rauchfuss and S. R. Wilson, *Inorg. Chem.*, 1995, **34**, 3072–3078.
57. H. Xu, Y. Deng, Z. Zhao, H. Xu, X. Qin and G. Chen, *Chem. Commun.*, 2014, **50**, 10468–10470.
58. F. Sun, J. Wang, H. Chen, W. Li, W. Qiao, D. Long and L. Ling, *ACS Appl. Mater. Interfaces*, 2013, **5**, 5630–5638.
59. L. Xiao, Y. Cao, J. Xiao, B. Schwenzer, M. H. Engelhard, L. V. Saraf, Z. Nie, G. J. Exarhos and J. Liu, *Adv. Mater.*, 2012, **24**, 1176–1181.
60. C. Lai, X. P. Gao, B. Zhang, T. Y. Yan and Z. Zhou, *J. Phys. Chem. C*, 2009, **113**, 4712–4716.
61. J. Guo, Z. Yang, Y. Yu, H. D. Abruña and L. A. Archer, *J. Am. Chem. Soc.*, 2013, **135**, 763–767.
62. J. Song, T. Xu, M. L. Gordin, P. Zhu, D. Lv, Y. B. Jiang, Y. Chen, Y. Duan and D. Wang, *Adv. Funct. Mater.*, 2014, **24**, 1243–1250.
63. P. Zhu, J. Song, D. Lv, D. Wang, C. Jaye, D. A. Fischer, T. Wu and Y. Chen, *J. Phys. Chem. C*, 2014, **118**, 7765–7771.
64. G. Zhou, E. Paek, G. S. Hwang and A. Manthiram, *Nat Commun*, 2015, **6**, 7760. DOI: 10.1038/ncomms8760.